

## Influence of ultrasonic and mechanochemical treatment on the electronic structure of functional composites of $\text{TiO}_2$ and $\text{ZrO}_2$

V.V.Zaika<sup>1</sup>, V.L.Karbivskii<sup>1,3</sup>, E.V.Sachuk<sup>2</sup>, L.I.Karbivska<sup>1</sup>,  
N.A.Zueva<sup>1</sup>, V.H.Kasiyanenko<sup>1</sup>, A.I.Sobolev<sup>1</sup>, S.I.Shulyma<sup>1</sup>,  
N.K.Shvachko<sup>1</sup>, V.O.Zazhigalov<sup>2</sup>

<sup>1</sup>G.V.Kurdyumov Institute for Metal Physics, National Academy of Sciences of Ukraine, 03680 Kyiv, Ukraine

<sup>2</sup>Institute for Sorption and Problems of Endoecology, 03164 Kyiv, Ukraine

<sup>3</sup>Leibniz Institute for Solid State and Materials Research,  
01068 Dresden, Germany

Received October 30, 2022

The effect of various methods, in particular, mechanochemical and ultrasonic treatment of  $\text{TiO}_2/\text{ZrO}_2$  composites, on the electronic structure was investigated. X-ray photoelectron spectroscopy (XPS) was used. XPS spectra were analyzed using an original technique for decomposing the spectra into components. We analyzed changes in the binding energies of the core electrons, the spin-orbital splitting, changes in the full width at half-maximum of the peaks, and relative changes in the intensity of the spectral components. It is shown that mechanochemical treatment of the  $\text{TiO}_2/\text{ZrO}_2$  composite leads to a significant increase in oxidation capacity compared to ultrasonic treatment. It was found that during ultrasonic treatment, compared to mechanochemical treatment, the content of the nanocrystalline X-ray amorphous phase of titanium oxide increases with a relative decrease in the X-ray amorphous phase of zirconium oxide. Both mechanochemical and ultrasonic treatments of the  $\text{TiO}_2/\text{ZrO}_2$  composite contribute to a more homogeneous composition compared to the original sample. During the composite treatment, part of the titanium oxide underwent a phase transition from anatase to rutile. Based on the analysis of X-ray photoelectron spectra, recommendations for the use of processing methods to obtain improved physical and chemical properties of composites are given.

**Keywords:** electronic structure, metal oxides, composites, mechanochemistry, ultrasonic treatment, chemical shift, oxidation.

**Вплив ультразвукової та механохімічної обробки на електронну будову функціональних композитів  $\text{TiO}_2$  та  $\text{ZrO}_2$ . В.В.Заїка, В.Л.Карбівський, О.В.Сачук, Л.І.Карбівська, Н.А.Зуєва, В.Х.Касіяненко, А.І.Соболєв, С.І.Шулима, Н.К.Швачко, В.О.Зажигалов**

Досліджено вплив різних методів, зокрема, механохімічної та ультразвукової обробки композитів  $\text{TiO}_2/\text{ZrO}_2$  на електронну структуру. Використано метод рентгенівської фотоелектронної спектроскопії (РФС). Аналіз РФС спектрів проводився з використанням оригінальної методики розкладання спектрів на компоненти. Проаналізовано зміни енергій зв'язку остових електронів елементів, спін-орбітального розщеплення елементів, зміни повної ширини на половині висоті піків, а також відносні зміни інтенсивності компонентів спектрів. Показано, що механохімічна обробка композиту  $\text{TiO}_2/\text{ZrO}_2$  призводить до значного збільшення окисної здатності порівняно з ультразвуковою обробкою. Встановлено, що в процесі ультразвукової обробки, порівнюючи з механохімічною, відбувається збільшення вмісту нанокристалічної рентгеноаморфної фази оксиду титану та відносне зменшення рентгеноаморфної фази цирконію. Як меха-

нохімічна, так і ультразвукова обробка композиту  $\text{TiO}_2/\text{ZrO}_2$  сприяють утворенню більш гомогенного складу оксидної суміші, порівнюючи з вихідним зразком. У процесі обробки композиту частинка оксиду титану зазнала фазового переходу від анатазу до рутилу. На основі аналізу рентгеноелектронних спектрів надано рекомендації щодо використання методів обробки для отримання покращених фізико-хімічних властивостей композитів.

### 1. Introduction

Among the binary oxides, the material based on  $\text{TiO}_2/\text{ZrO}_2$  is of special attention due to its large surface area, as well as mechanical strength and non-toxicity [1]. Composite materials based on  $\text{TiO}_2/\text{ZrO}_2$  are used for a wide range of applications, in particular, for heterogeneous catalysis, as sensors, solar energy converters, etc. [2]. The various functional properties of such materials depend significantly on the pre-treatment technology. Taking into account the conditions of synthesis and processing can lead to the necessary practical properties. At the same time, knowledge about the electronic structure provides a basis for spectrally directed synthesis of such materials. Considering the above, the study of the electronic structure of composite materials based on  $\text{TiO}_2/\text{ZrO}_2$  after various technological treatments is an important scientific task.

### 2. Experimental

Preparation of the oxide titanium-zirconium composition with molar ratio  $\text{TiO}_2/\text{ZrO}_2 = 1:1$  was carried out by mixing  $\text{TiO}_2$  and  $\text{ZrO}_2$  powders (oxides qualification "h"). The samples were subjected to mechanochemical treatment in a Fritsch Pulverisette-6 planetary ball mill at 550 rpm for 4 hours in air. For the synthesis, we used a milling beaker (200 ml) and  $\text{ZrO}_2$  balls (5 mm in diameter), the ratio of the weight of the balls to the weight of the oxide mixture (10 g sample weight) was 10:1.

Ultrasonic treatment of samples (10 g sample weight) was carried out in an aqueous medium (80 ml) for 1 h using a UZDN-2T dispersant, which operates in the acoustic cavitation mode with a frequency of 40 kHz. The temperature of the reaction medium was maintained at 80°C by circulating cold water around the reactor. After the ultrasonic treatment, the obtained samples were dried at 110°C in air.

X-ray photoelectron spectra of the samples were obtained using a JEOL-Japan XPS 2400 X-ray spectrometer. The working vacuum was no lower than  $10^{-7}$  Pa. Radiation from a magnesium anode with  $\text{Mg-K}\alpha$  line energy of 1253.6 eV was used. The energy

resolution was 0.1 eV. The spectra were calibrated against the C 1s line (284.0 eV), which is characteristic of hydrocarbons introduced from the atmosphere on the surface of solids.

### 3. Results and discussion

To estimate the distribution of chemical components in the surface layer of the composites, a quantitative analysis of samples was performed using the integral intensities of the XPS spectra of O 1s, Ti 2p<sub>3/2</sub> and Zr 3p<sub>3/2</sub>, taking into account the effective scattering cross-sections. Assuming that the yield depth for photoelectrons lies within 10 nm, the data in Table 1 characterize only the surface composition. It can be seen that each of the treatments leads to an increase in the oxygen concentration on the surface of the particles. Since the treated samples were dried at 110°C, and as a result there was an increase in the amount of oxygen, it can be concluded that the treatment process chemically binds additional oxygen. The mechanical treatment method results in a higher Ti/Zr ratio on the composite surface compared to the ultrasonic treatment. This feature can be explained by the higher atomic weight of zirconium oxide or the smaller particle size of zirconium oxide powder. Since mechanochemical treatment showed a greater amount of oxygen on the surface, it can be assumed that the mechanochemical treatment provides higher oxidizing ability.

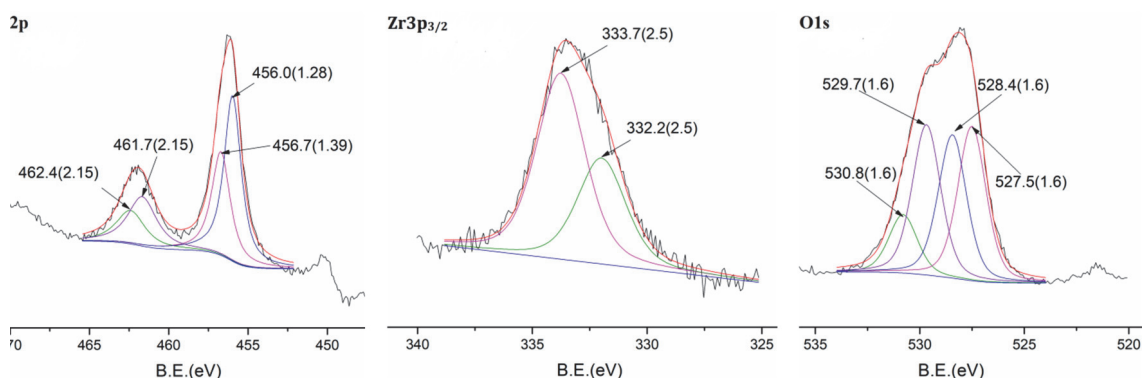
In order to describe the changes in the electronic structure of the composites, the method of decomposition of photoelectron spectra into components by chemical elements was used. The authors applied an original decomposition program [3]. The de-

Table 1. Chemical composition of the surface according to XPS data (at.%)

Element/Sample	O, %	Ti, %	Zr, %	Ti/Zr
Original sample	62.0	21.6	16.4	1.31
Mechanochemical treatment	65.8	18.4	15.8	1.16
Ultrasonic treatment	63.6	19.2	17.2	1.12

Table 2. The ratio of particle areas relative to the original sample

	Ti 2p <sub>3/2</sub> , eV	Zr 3p <sub>3/2</sub> , eV	$\Delta E(\text{Ti})$ , eV	$\Delta E(\text{Zr})$ , eV	$S_0/S_p (\text{Ti } 2p)$	$S_0/S_p (\text{Zr } 3p)$
Original sample	456.21	333.09	—	—	—	—
Mechanochemical treatment	458.07	331.87	1.86	1.22	6.42	3.39
Ultrasonic treatment	456.72	331.67	0.51	1.42	1.67	4.14

Fig. 1. XPS spectra of the original composite sample  $\text{ZrO}_2/\text{TiO}_2$ .

composition algorithm implied taking into account 5 parameters for each component of the spectrum. The actual minimum in the multiparameter problem was achieved by gradient descent and reaching the agreement between the calculated and experimental data with the minimum permissible discrepancy parameter. For titanium spectral lines, the initial values of the full-width at half-maximum (FWHM) were taken from [4]. The corresponding FWHM value for the zirconium  $\text{ZrO}_2$  lines was taken from [5]. The spin orbital splitting parameter for the  $2p$  states of titanium in  $\text{TiO}_2$  was assumed to be 5.7 eV according to the NIST database [6] and corresponded to the experimentally measured one.

In this paper, the FWHM ratio for  $\text{TiO}_2$   $2p_{1/2}/\text{TiO}_2$   $2p_{3/2}$  was about 1.7, whereas for metallic titanium this ratio is approximately equal to 1.32 [7]. For a similar composite  $\text{TiO}_2$   $2p_{1/2}/\text{TiO}_2$   $2p_{3/2}$ , Bagus et al. [8] obtained an FWHM ratio of about 2; this feature is related to the broadening of the  $\text{Ti } 2p_{1/2}$  peak due to a large number of unresolved final states.

The decomposition into components of X-ray photoelectron spectra of these composites showed (Fig. 1) that there are two different states for titanium and zirconium. Taking into account that the initial sample was obtained by mixing  $\text{ZrO}_2$  and  $\text{TiO}_2$  powders, the appearance of several peaks in the spectra of the core electrons can be ex-

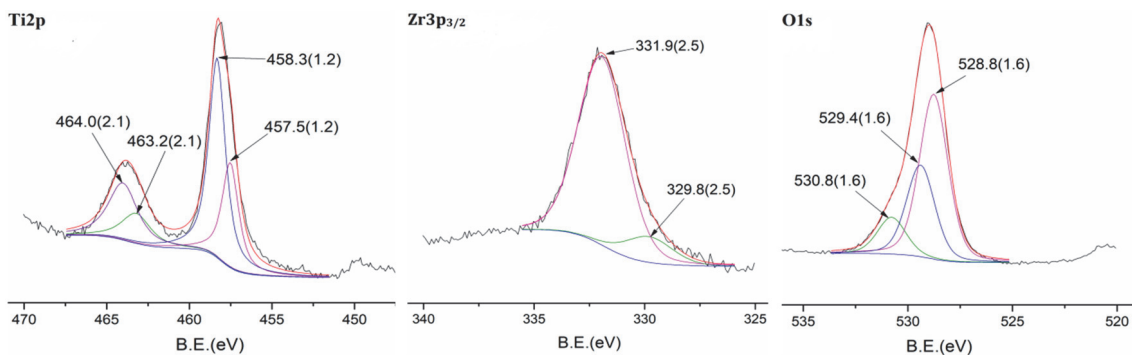
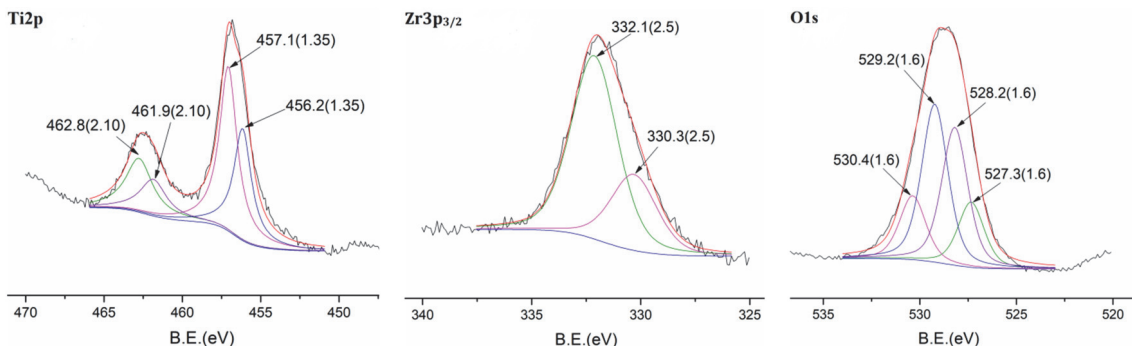
plained by different crystallochemical states for the chemical elements in the powders. Thus, the four components of the decomposed spectrum of oxygen correspond not only to different crystallochemical phases of oxides but also to different aggregation states — amorphous or crystalline. The dependence of the chemical shift on the particle size was studied in [9]. For metals, a logarithmic dependence of the chemical shift of an X-ray photoelectron line  $\Delta E_b$  (eV) on the area of particles is established, where  $S_{part}$  is the area of particles on the surface, and  $S_0$  is the area of particles that do not experience a dimensional energy shift

$$\Delta E_b = \ln \left( \frac{S_0}{S_{part}} \right). \quad (1)$$

Using this formula for spectra of titanium and zirconium, the ratio between the areas of particles relative to the original sample was established (Table 2).

In [10], using the X-ray diffraction (XRD) method, it was found that after similar treatments of such composites, the samples became X-ray amorphous. In [11], the amorphous phase of similar composites was obtained using the sol gel method. Apparently, the samples are partially transformed into an amorphous phase after treatment.

We can also assume that the components of the decomposition spectra reflect the crystalline and amorphous states of the

Fig. 2. XPS spectra of the composite  $\text{ZrO}_2/\text{TiO}_2$  after mechanochemical treatment.Fig. 3. XPS spectra of composite  $\text{ZrO}_2/\text{TiO}_2$  after ultrasonic treatment.

phases in addition to the chemical state of the element. Considering that the precursors for the synthesis were polycrystalline powders of metal oxides, most of the sample should have remained in the primary crystalline phase. Consequently, the lower intensity peaks should correspond to the amorphous phase in the treated composites. When passing from the original sample to the treated sample, a significant change in the intensity of the decomposition components of the  $2p$  titanium spectra is observed. The high-energy  $\text{Ti } 2p_{3/2}$  component increases its intensity by almost a factor of 2 upon going to treated composites. Based on the ratio of integral intensities of the spectral components, it was shown that the content titanium is significantly higher than the content of zirconium on the surface.

For the treated composites, there is a decrease in the zirconium p-states binding energy, which may indicate a decrease in the number of bonds between zirconium and oxygen atoms as well as some increase in the electron density of the zirconium atoms (Table 3). The increase in the binding energy for the titanium components indicates the opposite effect, hence, the electron density decreases in titanium atoms.

Table 3. Binding energy of decomposition component peaks for titanium and zirconium

	$\text{Ti } 2p_{3/2}$ , eV	$\text{Zr } 3p_{3/2}$ , eV	$\text{O } 1s$ , eV
Original sample	456.0	332.2	527.5
	456.7	333.7	528.4
			529.7
			530.8
Mechanochemical treatment	457.5	329.8	528.8
	458.3	331.9	529.4
			530.8
Ultrasonic treatment	456.2	330.3	527.3
	457.1	332.1	528.2
			529.2
			530.4

The most striking metamorphosis is observed in the  $1s$  spectra of oxygen. For the original sample, two peaks are observed in the oxygen spectrum (Fig. 1) due to the mixing of the two oxides. When the spectrum is decomposed into components having a characteristic half-width, four peaks are obtained, which is consistent with the above statement about the presence of various

Table 4. Spin-orbital splitting for Ti 2p

Original sample	5.78 eV
Mechanochemical treatment	5.74 eV
Ultrasonic treatment	5.93 eV

phases with the participation of oxygen. The different treatments of the composite lead to a significant narrowing of the lines of the oxygen spectrum due to an increase in its concentration on the surface of the samples. Apparently, both treatments contribute to the formation of a more homogeneous state of the composite compared to the original sample.

The change in the spin-orbital splitting indicates a significant change in the first coordination sphere of the element, which may be associated with the phase transition during the treatment of the composite (Table 4). Based on the spin-orbital splitting, the original sample of titanium oxide was in the anatase phase. The spin-orbital splitting for it was 5.78 eV. In [7] this value was reported as 5.77 eV for the titanium oxide in the anatase phase. Table 4 shows the spin-orbital splitting of 5.74 eV after the mechanical treatment, which corresponds to the anatase phase.

An increase in the spin-orbit splitting by 0.15 eV (Table 4) indicates a possible phase transition. Thus, it can be assumed that after the ultrasonic treatment, a part of the sample underwent a transformation of the atomic structure in the form of an anatase-rutile phase transition.

#### 4. Conclusions

The effect of different treatment methods, in particular, mechanochemical and ultrasonic treatment of  $\text{TiO}_2/\text{ZrO}_2$  composites, on the electronic structure was investigated. Both used treatment methods lead to an increase in the amount of surface oxygen. With mechanochemical treatment of the samples, the increase in oxygen is 3.8 at. % and with ultrasonic treatment it is 1.6 at. %. Thus, the mechanical treatment of the  $\text{TiO}_2/\text{ZrO}_2$  composite leads to a significant increase in oxidative capacity compared to the ultrasonic treatment.

In the ultrasonic treatment process there is an increase in the contribution of surface atoms of titanium and a decrease in the contribution of surface atoms of zirconium into the integral intensities of the spectra of metals. This effect can be attributed to the fact that during ultrasonic treatment, in comparison with mechanochemical treatment, there is an increase in the content of the nanocrystalline X-ray amorphous phase of titanium oxide and a relative decrease in the content of the amorphous phase of zirconium.

Both mechanochemical and ultrasonic processing of the  $\text{TiO}_2/\text{ZrO}_2$  composite contributes to a greater homogeneity of the composite compared to the original sample. During the composite processing, a part of the titanium oxide undergoes a phase transition from anatase to rutile.

#### References

1. A.Kubiak, K.Siwinska-Ciesieleszyk, T.Jesionowski, *Materials*, **11**, 2295 (2018).
2. M.S.Sanu, G.Gejo, M.S.Sajna et al., *Appl. Surf. Sci. Adv.*, **6**, 100173 (2021).
3. A.P.Shpak, V.L.Karbivskyy, L.P.Klyuenko, M.V.Shapochkin, Computer Processing, Decomposition, Separation of Instrumental Broadening and Visualisation of X-ray Spectra, NTUU KPI, Kiev (2001) [in Ukraine].
4. N.Ikeo, Y.Iijima, N.Niimura et al., Handbook of X-ray Photoelectron Spectroscopy, JEOL Ltd, Tokyo (1991).
5. B.Vincent Crist, Handbook of Monochromatic XPS Spectra Volume Two-Commercially Pure Binary Oxide, 2, XPS International LLC (2018).
6. NIST X-ray Photoelectron Spectroscopy Database, NIST Standard Reference Database Number 20, National Institute of Standards and Technology, Gaithersburg MD, 20899 (2000).
7. M.C.Biesinger, L.W.M.Lau, A.R.Gerson, R.S.C.Smart, *Appl. Surf. Sci.*, **257**, 887 (2010).
8. P.S.Bagus, C.J.Nelin, C.R.Brundle, S.A.Chambers, *J.Phys.Chem.C*, **123**, 7705 (2019).
9. A.I.Kovalev, D.L.Wainstein, A.Y.Rashkovskiy et al., *Surf.Interface Anal.*, **42**, 850 (2010).
10. M.Stubicar, V.Bermanec, N.Stubicar et al., *J. Alloys and Compd.*, **316**, 316 (2001).
11. M.Manriquez, T.Lopez, R.Gomez, J.Navarrete, *J.Mol.Catal.A Chem.*, **220**, 229 (2004).